Letter Report

Yucca Mountain Environmental Monitoring Systems Initiative
Air Quality Scoping Study for Crater Flat, Nye County, Nevada

prepared by

Johann Engelbrecht, Ilias Kavouras, Dave Campbell,
Scott Campbell, Steven Kohl and David Shafer
Desert Research Institute
Nevada System of Higher Education

submitted to

Nevada Site Office
National Nuclear Security Administration
U.S. Department of Energy
Las Vegas, Nevada

August 2008

CONTENTS

LIST OF FIGURES

LIST OF TABLES

INTRODUCTION

The Desert Research Institute (DRI) is performing a scoping study as part of the U.S. Department of Energy's Yucca Mountain Environmental Monitoring Systems Initiative (EMSI). The main objective is to obtain baseline air quality information for Yucca Mountain and an area surrounding the Nevada Test Site (NTS).

Air quality and meteorological monitoring and sampling equipment housed in a mobile trailer (shelter) (cover page figure) is collecting data at eight sites outside the NTS, including Ash Meadows National Wildlife Refuge (NWR), Beatty, Sarcobatus Flats, Rachel, Caliente, Pahranagat NWR, Crater Flat, and Tonopah Airport, and at four sites on the NTS (Engelbrecht *et al*., 2007a-d). The trailer is stationed at any one site for approximately eight weeks at a time.

This letter report provides a summary of air quality and meteorological data, on completion of the site's sampling program.

SITE LOCATION AND CHARACTERISTICS

Crater Flat is adjacent to the proposed Yucca Mountain nuclear repository, just outside of the NTS boundaries. The existing plans for the facility indicate that a railroad and heavy-haul roads, to transfer nuclear waste to the repository, will pass through Crater Flat. The sampling site is located 15 miles southeast of the town of Beatty, and about 6 miles east of U.S. Route 95. It is about 90 miles northwest of Las Vegas (Figure 1).
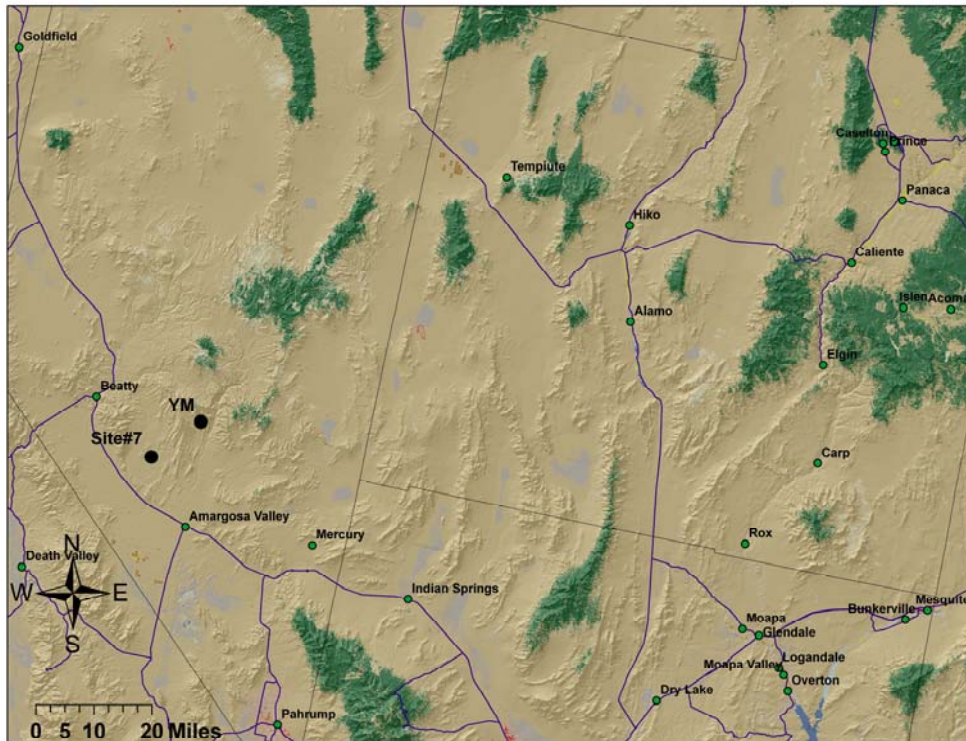
Figure 1. Southern Nevada map showing the location of Site #7 (at Crater Flat), Nevada Test Site, and Yucca Mountain. The map background is land use and land cover from the 2001 National Land Cover Database.

The mobile trailer was located inside a fenced area at well VH-1, on the edge of the Yucca Mountain Repository Facility Program area. Monitoring of PM_{10}, $PM_{2.5}$, and meteorological conditions was carried out from May 25, 2007, to August 29, 2007. Because of the remote location of the site, instrumentation that required 120-volt AC power (TEOMs) did not run. The portable DUSTTRAK, meteorological equipment, and integrated PM samplers were run from 12-volt batteries, charged by solar panels.

Table 1. Longitude, latitude, and elevation of the mobile trailer location at Site #7 (Crater Flat).

Site	Crater Flat
Latitude	36° 47' 31.81"
Longitude	116° 33' 9.75"

AEROSOL SAMPLING AND MONITORING

Filter Sampling

Sampler Description and Procedures

BGI, Inc., PQ100 and PQ200 Ambient $PM_{2.5}$ Federal Reference Method (FRM) samplers were used to collect 24-h integrated PM_{10} and $PM_{2.5}$ samples. Figure 2 shows the PQ100 and PQ200 in the mobile trailer (left) and the PM_{10} sampling inlets on the top of the trailer (right). Both the PQ100 (Designation No. RFPS-1298-124) and PQ200 (Designation No. RFPS-0498-116) samplers are designed to meet the criteria for collecting 24-h samples of ambient aerosol according to the U.S. National Ambient Air Quality Standards (NAAQS).

Figure 2.   Photographs of PQ100 (green/gray box in left photo), PQ200 (white box in left photo) and their sampling inlets (right photo).

Figure 3 shows a schematic drawing of the samplers. Particles with aerodynamic diameter larger than 10 μm are removed by impaction by the size selective inlet, while the smaller particles remain airborne. The PM_{10} fraction is collected by a filter located downstream of the size selective inlet. For the collection of $PM_{2.5}$, particles in the range between 2.5 and 10 μm were removed by the Very Sharp Cut Cyclone (VSCC) (U.S.

Environmental Protection Agency [EPA] Equivalent Designation No. EQPM-0202-142), then collected on a filter.
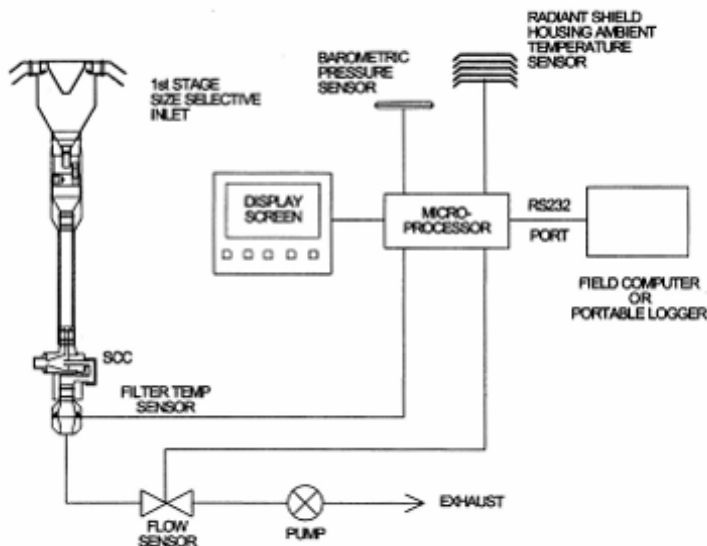
Figure 3.   A diagrammatic representation of the BGI $PM_{2.5}$ sampler showing the PM_{10} size selective impactor head as the first stage followed by a $PM_{2.5}$ VSCC. This configuration can be readily modified to a PM_{10} sampler by removal of the VSCC.

For both PQ100 and PQ200, samples were collected at a volumetric flow rate of 16.67 liters/min. The flow rate is controlled to ±2 percent precision with a mass flow controller. The actual ambient temperature and barometric pressure, filter temperature and pressure, and anomalies (if any) were recorded by a microprocessor. The sampler was equipped to operate from an internal 12-volt DC battery. The battery was normally recharged from 120-volt AC. Alternatively, a 32-watt solar panel with an additional external ballast battery was installed to provide power for periods without electricity. Two sets of PQ100 and PQ200 samplers were installed in the mobile trailer. PM_{10} and $PM_{2.5}$ samples were collected on filters in numbered cassettes, labeled TT (for PM_{10} Teflon), FT (for $PM_{2.5}$ Teflon), TQ (for PM_{10} Quartz), and FQ (for $PM_{2.5}$ Quartz). Each filter cassette was loaded with a pre-weighed 46.2-mm-diameter PTFE (Teflon) membrane filter (Whatman # 7592-004) or 47-mm quartz fiber (Pallflex #2500QAT-UP) filter. The Teflon membrane collected particles for gravimetric analysis, light absorption by densitometry, and elements by X-ray fluorescence spectrometry. Quartz fiber filters were used for measurement of water-soluble ions by atomic absorption spectrometry, ion chromatography, and automated colorimetry, and also for measurement of carbon species by thermal optical reflectance.

Operation, calibration, and maintenance of PQ100 and PQ200 particulate samplers are described in standard operating procedure DRI SOP # 1-211.2 "BGI PQ100 PM10 and PQ200 PM2.5 REFERENCE SAMPLERS FOR THE YUCCA MOUNTAIN AIR QUALITY PROGRAM." Flow calibration and leak tests (only for PQ200) were performed on the day of installation (May 25, 2007). The leak check was performed according to the manufacturer's operational instruction manual only for PQ200; no procedure exists from the manufacture for the PQ100. The flow rates were set according to a BGI Tri-Cal NIST

traceable standard. The sampler was then placed in "calibration" or "run" mode and a one-point calibration verification or one-point flow-rate verification performed. Aerosol samples were collected on a 1-in-6-day schedule. Audits of the flow and leak tests were done onsite at the beginning and end of the monitoring campaign. Teflon and quartz filters were prepared and assembled in their filter holders by the Desert Research Institute's (DRI) Environmental Analysis Facility (EAF) in Reno and shipped to DRI's facilities in Las Vegas. The filters were kept at -4°C and transported to the field in a cryo-cooler. Exposed filters were also stored at -4°C in Las Vegas. Upon completion of the monitoring period at the site, all filters were shipped to the EAF in Reno.

Gravimetry

Table 2 shows mass concentrations (and uncertainty) of filters collected at Crater Flat. PM_{10} mass concentrations varied from 5.24 μg/m^3 to 27.62 μg/m^3, while $PM_{2.5}$ mass concentrations ranged from 2.99 μg/m^3 to 14.31 μg/m^3. Similar temporal trends were observed for both PM_{10} and $PM_{2.5}$. In all cases, 24-h PM_{10} and $PM_{2.5}$ levels were significantly lower than the NAAQS as recently revised by EPA (24-h PM_{10}: 150 μg/m^3, 24-h $PM_{2.5}$: 35 μg/m^3; Annual $PM_{2.5}$: 15 μg/m^3) (Figure 4). On average, fine particulates ($PM_{2.5}$) accounted for approximately half of PM_{10} ($PM_{2.5}/PM_{10}$ ratio of 0.49) (Figure 5). This value indicated the significant contribution of coarse particles probably due to the emissions from nearby unpaved roads that connect several mine operations with U.S. Route 95. The possible contributions of smoke from a human-ignited fire (Zaca) in Santa Barbara, California, may have contributed to high PM_{10} and $PM_{2.5}$ levels. The fire ignited on July 4, 2008, and lasted more than two months.

Table 2. Collection days, filter numbers, mass, and uncertainties by gravimetric analysis, and associated flags of samples from Site #7 (Crater Flat).

Date	No	Type	Mass (μg/m^3)	Uncertainty (μg/m^3)	Flags
5/30/2007	085	PM_{10}	-99.0000	-99.0000	V: invalid (void) analysis result; T: sampling time error
		$PM_{2.5}$	6.2422	0.4456	
6/05/2007	087	PM_{10}	27.6206	0.6986	
		$PM_{2.5}$	14.3154	0.5148	
6/11/2007	088	PM_{10}	15.3910	0.5269	N: foreign substance on sample
		$PM_{2.5}$	9.0266	0.4641	
6/17/2007		PM_{10}	13.1448	0.5020	
		$PM_{2.5}$	5.5347	0.4419	
6/23/2007		PM_{10}	-99.0000	-99.0000	V: invalid (void) analysis result
		$PM_{2.5}$	-99.0000	-99.0000	V: invalid (void) analysis result
6/29/2007		PM_{10}	11.6889	0.4873	
		$PM_{2.5}$	5.9068	0.4436	
7/05/2007		PM_{10}	8.4443	0.4598	
		$PM_{2.5}$	4.0349	0.4352	
7/11/2007		PM_{10}	18.7188	0.5683	N: foreign substance on sample
		$PM_{2.5}$	8.2779	0.4585	
7/17/2007		PM_{10}	12.7288	0.4977	N: foreign substance on sample
		$PM_{2.5}$	7.0715	0.4504	

Table 3. Collection days, filter numbers, mass, and uncertainties by gravimetric analysis, and associated flags of samples from Site #7 (Crater Flat) (continued).

| Date	No	Type	Mass (μg/m^3)	Uncertainty (μg/m^3)	Flags
7/23/2007		PM_{10}	23.5827	0.6367	N: foreign substance on sample
		$PM_{2.5}$	8.2363	0.4582	
7/29/2007		PM_{10}	14.3095	0.5145	
		$PM_{2.5}$	7.9867	0.4565	
8/04/2007		PM_{10}	21.7554	0.6101	N: foreign substance o n sample
		$PM_{2.5}$	11.6473	0.4869	
8/10/2007		PM_{10}	13.1448	0.5020	
		$PM_{2.5}$	6.0732	0.4445	
8/16/2007		PM_{10}	13.0616	0.5011	
		$PM_{2.5}$	9.9834	0.4719	
8/22/2007		PM_{10}	19.7171	0.5817	
		$PM_{2.5}$	8.1981	0.4581	
8/28/2007		PM_{10}	5.2413	0.4403	
		$PM_{2.5}$	2.9950	0.4318	
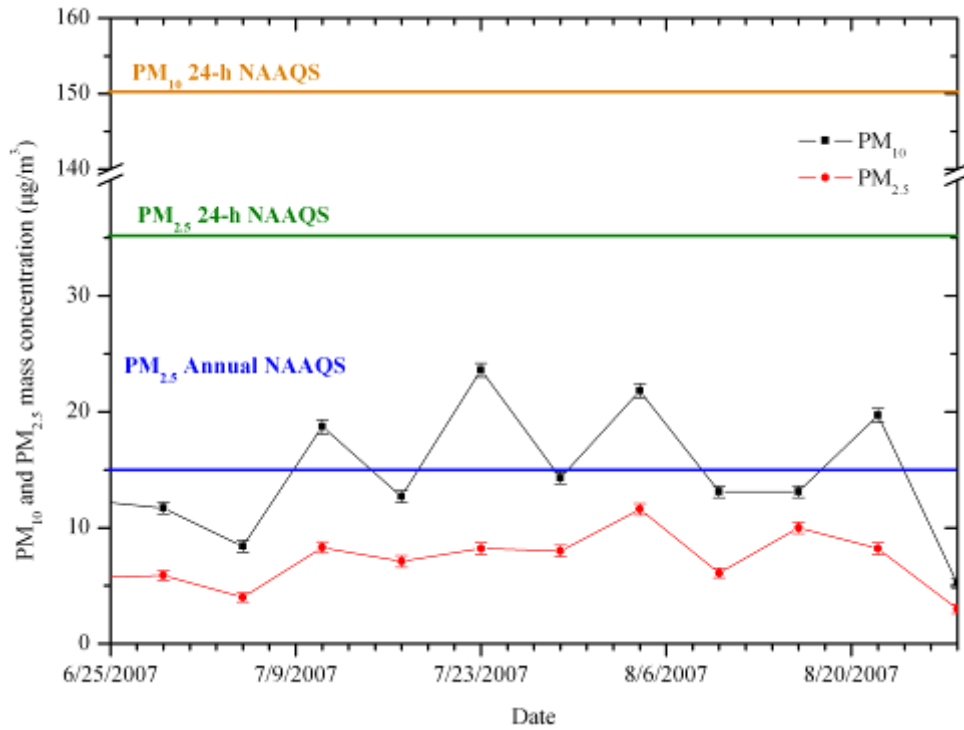
Figure 4. Time series of PM_{10} and $PM_{2.5}$ mass concentrations ($\pm$ uncertainty) at Site #7 (Crater Flat).
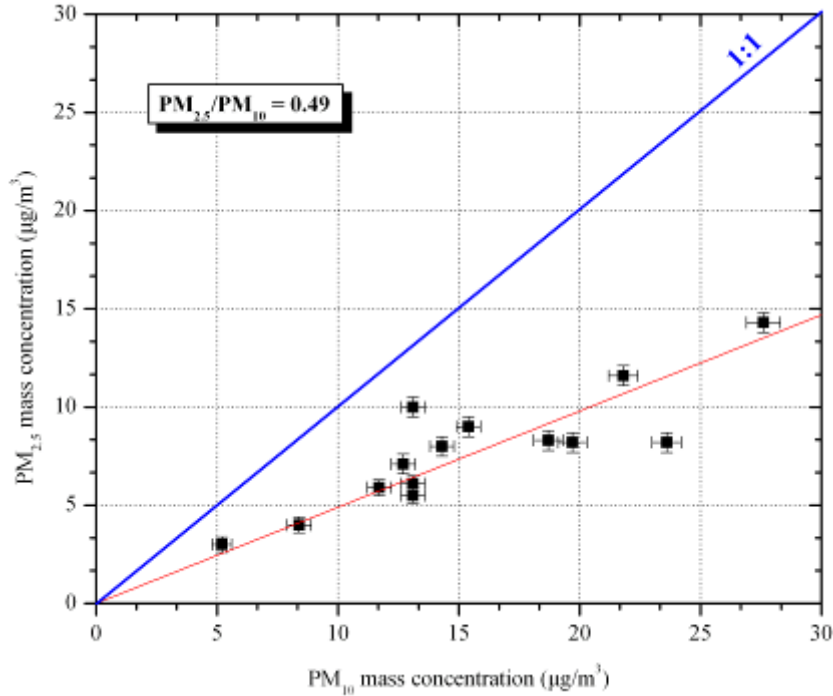
Figure 5.   Relationship between mean (± uncertainty) daily $PM_{2.5}$ and PM_{10} at Crater Flat.

Chemical Analysis

Table 3 shows the chemical content of PM_{10} and $PM_{2.5}$ samples collected on June 5, 2007 and July 29, 2007. Chemical analysis included elements (from sodium to uranium) with X-ray fluorescence spectrometry (XRF), major anions (sulfate, nitrate, and chloride) by ion chromatography (IC), major cations (sodium, potassium) by atomic absorption (AA), particulate ammonium by automated colorimetry (AC), and elemental and organic carbon by thermal optical reflectance (TOR).

Table 4.   Results of the chemical analysis for selected filters from Crater Flat. Chemical components with concentrations higher than twice the uncertainty are in bold, while those with concentrations lower than twice the uncertainty are in italics. Concentrations are in $\mu g/m^3$.

DATE	6/05/2007				7/29/2007			
SIZE	PM_{10}		$PM_{2.5}$		PM_{10}		$PM_{2.5}$	
	Conc.	Uncer.	Conc.	Uncer.	Conc.	Uncer.	Conc.	Uncer.
Mass	**27.6206**	**0.6986**	**14.3154**	**0.5148**	**14.3095**	**0.5195**	**7.9867**	**0.4565**
Chloride, Cl^-	**0.0986**	**0.0306**	*0.028*	*0.0295*	*0.0504*	*0.0297*	*0*	*0.0294*
Nitrate, NO_3^-	**0.7898**	**0.0389**	**0.1817**	**0.0301**	**0.8003**	**0.0391**	**0.256**	**0.0307**
Sulfate, SO_4^{2-}	**1.7218**	**0.0476**	**1.1772**	**0.039**	**1.5718**	**0.0451**	**1.3291**	**0.0413**
Ammonium, NH_4^+	**0.4994**	**0.0345**	**0.4269**	**0.0333**	**0.5252**	**0.035**	**0.4567**	**0.0338**
Sodium, Na^+	**0.2661**	**0.0086**	**0.05**	**0.0057**	**0.2718**	**0.0087**	**0.1657**	**0.0069**
Magnesium, Mg^{2+}	**0.12**	**0.0034**	**0.0319**	**0.0015**	**0.0562**	**0.0019**	**0.0281**	**0.0014**
Potassium, K^+	**0.2997**	**0.008**	**0.0727**	**0.0035**	**0.0972**	**0.0038**	**0.0637**	**0.0033**
Calcium, Ca_{2+}	**3.0348**	**0.0754**	**0.41**	**0.0183**	**0.4056**	**0.0182**	**0.1425**	**0.0157**
OC1	**0.2897**	**0.1142**	**0.5678**	**0.2211**	**0.4678**	**0.1826**	**1.0175**	**0.3951**

Table 5. Results of the chemical analysis for selected filters from Crater Flat. Chemical components with concentrations higher than twice the uncertainty are in bold, while those with concentrations lower than twice the uncertainty are in italics. Concentrations are in μg/m^3 (continued).

DATE	6/05/2007				7/29/2007			
SIZE	PM$_{10}$		PM$_{2.5}$		PM$_{10}$		PM$_{2.5}$	
	Conc.	Uncer.	Conc.	Uncer.	Conc.	Uncer.	Conc.	Uncer.
OC2	**0.4734**	**0.1263**	**0.4045**	**0.1126**	**0.9596**	**0.2273**	**1.0903**	**0.255**
OC3	**1.2018**	**0.2343**	**0.5545**	**0.1764**	**1.059**	**0.2203**	**0.7917**	**0.1958**
OC4	**0.9126**	**0.1081**	**0.5315**	**0.0765**	**0.5889**	**0.0809**	**0.3922**	**0.0667**
Pyrolyzed OC-TT	**1.5083**	**0.5148**	**1.1956**	**0.4087**	**0.4746**	**0.1658**	**0.2594**	**0.0958**
Pyrolyzed OC-Op	**1.531**	**0.5445**	**1.1887**	**0.4234**	**0.3906**	**0.1435**	**0.1357**	**0.0607**
Total OC	**4.4084**	**0.4516**	**3.247**	**0.366**	**3.4659**	**0.3816**	**3.4274**	**0.379**
EC1	**1.326**	**0.3031**	**1.0749**	**0.2463**	**0.5904**	**0.1372**	**0.348**	**0.0839**
EC2	**0.205**	**0.0801**	**0.1139**	**0.053**	**0.096**	**0.0484**	**0.0461**	**0.0383**
EC3	**0.0179**	**0.0115**	**0.0069**	**0.0115**	**0**	**0.0115**	**0**	**0.0115**
Total EC	**0.0179**	**0.044**	**0.0069**	**0.0439**	**0.2957**	**0.0717**	**0.2583**	**0.0662**
Total Carbon	**5.3485**	**0.5456**	**3.3492**	**0.3918**	**3.7851**	**0.424**	**3.6857**	**0.4166**
Carbonate Carbon (CO$_3^{2-}$)	**0.9221**	**0.3424**	*0.0953*	*0.2166*	*0.0235*	*0.2149*	*0*	*0.2149*
Sodium, Na	**0.2085**	**0.0835**	*0.1068*	*0.0819*	*0.1549*	*0.0827*	*0.0631*	*0.0813*
Magnesium, Mg	**0.3547**	**0.0453**	**0.2196**	**0.0443**	**0.1242**	**0.0436**	**0.0436**	**0.0432**
Aluminum, Al	**1.1168**	**0.0257**	**0.6696**	**0.0168**	**0.4276**	**0.0124**	**0.2063**	**0.009**
Silicon, Si	**2.9874**	**0.0646**	**1.8426**	**0.0408**	**1.0569**	**0.0248**	**0.496**	**0.0141**
Phosphorous, P	**0.0131**	**0.003**	**0.0108**	**0.003**	**0.0231**	**0.003**	**0.0177**	**0.003**
Sulfur, S	**0.3513**	**0.0147**	**0.3873**	**0.0152**	**0.4995**	**0.0167**	**0.4579**	**0.0161**
Chlorine, Cl	**0.0158**	**0.0016**	**0.0088**	**0.0016**	**0.0083**	**0.0016**	**0.0044**	**0.0016**
Potassium, K	**0.585**	**0.012**	**0.3554**	**0.0074**	**0.2185**	**0.0047**	**0.0972**	**0.0025**
Calcium, Ca	**1.0629**	**0.0215**	**0.5308**	**0.0109**	**0.4111**	**0.0086**	**0.1653**	**0.0039**
Scandium, Sc	*0*	*0.0058*	*0*	*0.0058*	*0*	*0.0058*	*0*	*0.0058*
Titanium, Ti	**0.0745**	**0.0019**	**0.0463**	**0.0015**	**0.04**	**0.0014**	**0.0165**	**0.0012**
Vanadium, V	**0.0016**	**0.0001**	**0.0007**	**0.0001**	**0.0012**	**0.0001**	**0.0008**	**0.0001**
Chromium, Cr	*0*	*0.001*	*0*	*0.001*	*0*	*0.001*	*0*	*0.001*
Manganese, Mn	**0.0179**	**0.0022**	**0.0122**	**0.0022**	**0.0071**	**0.0021**	**0.0053**	**0.0021**
Iron, Fe	**0.7335**	**0.0152**	**0.422**	**0.0091**	**0.426**	**0.0092**	**0.1505**	**0.0043**
Cobalt, Co	*0*	*0.0001*	*0*	*0.0001*	*0*	*0.0001*	*0*	*0.0001*
Nickel, Ni	*0*	*0.0006*	*0*	*0.0006*	*0*	*0.0006*	*0*	*0.0006*
Copper, Cu	**0.0049**	**0.0009**	**0.0022**	**0.0009**	**0.0062**	**0.0009**	**0.0028**	**0.0009**
Zinc, Zn	**0.004**	**0.0009**	**0.0019**	**0.0009**	**0.003**	**0.0009**	**0.0019**	**0.0009**
Gallium, Ga	*0*	*0.0031*	*0*	*0.0031*	*0.0009*	*0.0031*	*0.0017*	*0.0031*
Arsenic, As	*0*	*0.0001*	*0*	*0.0001*	*0*	*0.0001*	*0*	*0.0001*
Selenium, Se	*0*	*0.0021*	*0.0007*	*0.0021*	*0.0001*	*0.0021*	*0.0004*	*0.0021*
Bromine, Br	*0.0025*	*0.0015*	*0.0015*	*0.0015*	*0.0026*	*0.0015*	*0.005*	*0.0015*
Rubidium, Rh	*0.0029*	*0.0011*	*0.0022*	*0.0011*	*0.0011*	*0.0011*	*0.0006*	*0.0011*
Strontium, Sr	**0.0115**	**0.002**	*0.006*	*0.002*	*0.0041*	*0.002*	*0.0017*	*0.002*
Yttrium, Y	*0.0001*	*0.0015*	*0.0008*	*0.0015*	*0.001*	*0.0015*	*0.0008*	*0.0015*
Zirconium, Zr	*0.0035*	*0.0035*	*0*	*0.0034*	*0.0002*	*0.0034*	*0.0006*	*0.0034*
Niobium, Nb	*0*	*0.0026*	*0*	*0.0026*	*0*	*0.0026*	*0*	*0.0026*
Molybdenum, Mo	*0*	*0.0024*	*0*	*0.0024*	*0*	*0.0024*	*0*	*0.0024*

Table 6. Results of the chemical analysis for selected filters from Crater Flat. Chemical components with concentrations higher than twice the uncertainty are in bold, while those with concentrations lower than twice the uncertainty are in italics. Concentrations are in µg/m^3 (continued).

DATE	6/05/2007				7/29/2007			
SIZE	PM$_{10}$		PM$_{2.5}$		PM$_{10}$		PM$_{2.5}$	
	Conc.	Uncer.	Conc.	Uncer.	Conc.	Uncer.	Conc.	Uncer.
Palladium, Pd	*0*	*0.0045*	*0*	*0.0045*	*0.0001*	*0.0045*	*0*	*0.0045*
Silver, Ag	*0*	*0.0041*	*0*	*0.0041*	*0*	*0.0041*	*0.0016*	*0.0041*
Cadmium, Cd	*0*	*0.0052*	*0*	*0.0052*	*0*	*0.0052*	*0*	*0.0052*
Indium, In	*0.0004*	*0.003*	*0*	*0.003*	*0.0015*	*0.003*	*0*	*0.003*
Tin, Sn	*0*	*0.0039*	*0*	*0.0039*	*0.0006*	*0.0039*	*0.0025*	*0.0039*
Antimony, Sb	*0*	*0.0073*	*0*	*0.0073*	*0*	*0.0073*	*0*	*0.0073*
Cesium, Cs	*0*	*0.0012*	*0*	*0.0012*	*0*	*0.0012*	*0*	*0.0012*
Barium, Ba	*0*	*0.0006*	*0*	*0.0006*	*0*	*0.0006*	*0*	*0.0006*
Lanthanum, La	*0*	*0.0009*	*0*	*0.0009*	*0*	*0.0009*	*0*	*0.0009*
Cerium, Ce	*0*	*0.0013*	*0*	*0.0013*	*0*	*0.0013*	*0.0007*	*0.0013*
Samarium, Sa	*0*	*0.0018*	*0*	*0.0018*	*0.0009*	*0.0018*	*0*	*0.0018*
Europium, Eu	*0.0003*	*0.0064*	*0.0028*	*0.0064*	*0*	*0.0064*	*0*	*0.0064*
Terbium, Tb	*0*	*0.0024*	*0*	*0.0024*	*0*	*0.0024*	*0*	*0.0024*
Hafnium, Hf	*0*	*0.0139*	*0*	*0.0139*	*0*	*0.0139*	*0*	*0.0139*
Tantalum, Ta	*0*	*0.0117*	*0*	*0.0117*	*0*	*0.0117*	*0*	*0.0117*
Tungsten, W	*0.0087*	*0.0168*	*0.0018*	*0.0168*	*0.0058*	*0.0168*	*0.0026*	*0.0168*
Iridium, Ir	*0*	*0.0036*	*0*	*0.0036*	*0*	*0.0036*	*0*	*0.0036*
Gold, Au	*0*	*0.0078*	*0.0001*	*0.0078*	*0*	*0.0078*	*0*	*0.0078*
Mercury, Hg	*0*	*0.0024*	*0*	*0.0024*	*0*	*0.0024*	*0*	*0.0024*
Thallium, Th	*0*	*0.0025*	*0*	*0.0025*	*0*	*0.0025*	*0*	*0.0025*
Lead, Pb	*0*	*0.0025*	*0.0002*	*0.0025*	*0*	*0.0025*	*0*	*0.0025*
Uranium, U	*0*	*0.0041*	*0*	*0.0041*	*0*	*0.0041*	*0.0021*	*0.0041*

OC = organic carbon
EC = elemental carbon
OP = optical pyrolysis
TT = transmittance

With respect to the chemical composition of PM$_{10}$ and PM$_{2.5}$, the following patterns were observed:

- Sulfur (S) was mostly in the form of sulfate (SO$_4^{2-}$) with sulfate-to-sulfur ratio of 2.90 to 4.90. Sulfate and ammonium were almost entirely associated with fine particles, while less than 30 percent of nitrate (23% to 30%) was measured in PM$_{2.5}$. Ammonium-to-sulfate molar ratios varied from 1.55 to 1.93, suggesting that sulfate aerosols were mostly in the form of ammonium bisulfate, (NH$_4$)HSO$_4$ (Malm *et al.*, 2002). Nitrates appeared to be partially neutralized by ammonium in the fine particle mode, while coarse particles nitrates may be from evaporites in soils or the product of the reactions of nitric acid with soil dust elements such as Ca^{2+}, Mg^{2+}, Na$^+$, and K$^+$ (Lefer and Talbot, 2001).

- Carbonaceous aerosol was predominantly in fine particles. For PM$_{2.5}$, organic carbon (OC) concentrations accounted for 23 to 46 percent of particle mass, while very low

EC/OC ratios were indicative of the absence of high temperature combustion-related sources.

- Soluble potassium (K^+) accounted for 20 to 66 percent of total potassium in PM_{10} and for more than 50 percent of total potassium in $PM_{2.5}$. Soluble potassium in fine particles is a tracer of biomass burning, which suggested the significant impact of emissions from local and/or regional fire (prescribed or wildfire) events. On the other hand, salts in desert soil may be the source of soluble potassium that is mostly present in the coarse fraction. This was further supported by the estimates of nonsoil potassium $K_{non-soil}$ (K_{total}-(0.26 x [Al])) that were comparable to measured water-soluble K^+. Water soluble K^+ is also present as salts in soils.

- Ratios of Al/Si (0.37 to 0.40) K/Fe (0.51 to 0.80) were comparable to those determined for samples collected at the Interagency Monitoring of Protected Visibility Environments (IMPROVE) sites in the western United States (Al/Si: 0.31 to 0.43, K/Fe: 0.67 to 0.78, Al/Ca: 1.4 to 1.7) when soil dust was the major component of particulate matter (Kavouras *et al*., 2005).

The IMPROVE mass calculation was applied to reconstruct aerosol mass into five major species, namely sulfate, nitrate, organic, light-absorbing carbon, and soil. For this scheme, sulfate and nitrate are assumed to be in the forms of ammonium sulfate [$(NH_4)_2SO_4$] and ammonium nitrate [NH_4NO_3], respectively (Malm *et al*., 2004). Organic mass concentration [OMC] was estimated as [OMC] =1.4 x [OC], where [OC] is the organic carbon concentration. The 1.4 factor was used to estimate for elements not measured (mainly hydrogen and oxygen) in organic compounds (White and Roberts, 1977). Soil mass concentration [SOIL] was estimated as the sum of the elements present in the soil as oxides calculated as follows:

[SOIL] = 2.2 x [Al] + 2.49 [Si] + 1.63 x [Ca] + 2.42 x [Fe] + 1.94 x [Ti]. Therefore, the reconstructed aerosol mass was estimated as follows:

[Aerosol Mass] = (128/96) x [SO_4] + (80/62) x [NO_3] + EC+ [OMC] + [SOIL]

Figure 6 shows the reconstructed concentrations of ammonium sulfate, ammonium nitrate, organic carbon, elemental carbon, and soil for PM_{10} and $PM_{2.5}$ collected on June 5, 2007 and July 29, 2007 in Crater Flat. Considering the positive bias for organic carbon measurements:

- Reconstructed particle mass accounted for 83 to 95 percent of measured PM_{10} mass and for 101 to 119 percent of $PM_{2.5}$ mass.

- Carbonaceous aerosol (OMC and EC) appeared to account for 22 to 36 percent of PM_{10} and 32 to 63 percent of $PM_{2.5}$.

- Soil represented 37 to 49 percent of PM_{10} and about 29 to 56 percent of $PM_{2.5}$ mass, while sulfate contributed between 8 and15 percent on PM_{10} and 11 to 22 percent on $PM_{2.5}$ (Figure 6).

The differences of PM_{10} and $PM_{2.5}$ fractions are due to higher concentration of soil elements in the coarse fraction (particles with diameter between 2.5 and 10 μm). Higher $PM_{2.5}$ mass concentrations for July 29, 2007, may be attributed to increased concentrations of organic carbon and to a lesser extent on soil and sulfate concentrations.
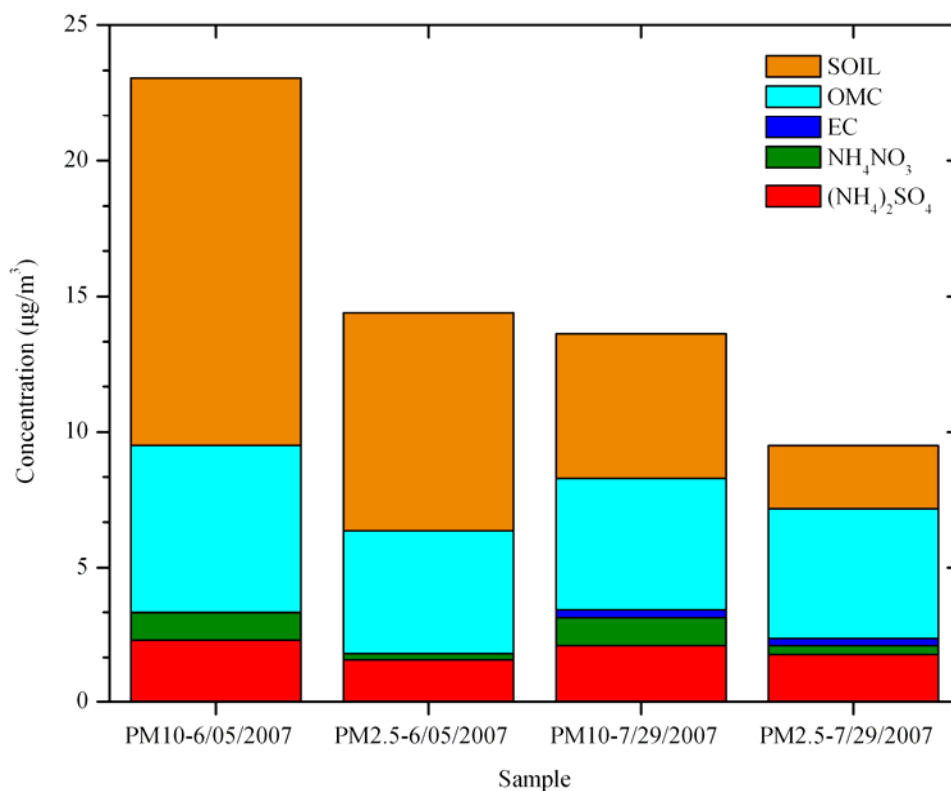
Figure 6. Reconstructed mass for PM10 and PM2.5 based on chemical composition.

Aerosol Monitoring

Monitor Description and Procedures

The DUSTTRAK™ Aerosol Monitors from TSI continuously measured PM_{10} and $PM_{2.5}$ mass concentrations (Figure 7). They are portable, battery operated laser photometers that provide measurements of particle mass, based on light scattering. Atmospheric aerosol passes through a size selective inlet (either PM_{10} or $PM_{2.5}$) and is directed to an optics chamber at a flow rate of 1.7 l/min. The light source is a laser diode that emits light at a wavelength of 780 nm. Sampled aerosol is drawn into the sensing chamber where it is illuminated with a narrow beam of laser light. Light scattered by aerosol particles is collected by a set of lenses and focused onto the photodetector. The detector signal is proportional to the amount of scattered light, which is proportional to the mass concentration of the aerosol. Voltage is read by the processor and multiplied by an internal calibration constant to yield mass concentration. The calibration constant is pre-set by the manufacturer for scattering characteristics of the respirable mass of ISO 12103-1, Al test dust. Local variations in aerosol particle size distribution and composition relative to this standard may result in differences in the actual response factor of the instrument. The operation, calibration, and maintenance of the DUSTRAK is described in DRI SOP 1.211-2 "TSI INCORPORATED MODEL 8520 DUSTTRAK AEROSOL MONITOR FOR THE YUCCA MOUNTAIN AIR QUALITY PROGRAM."
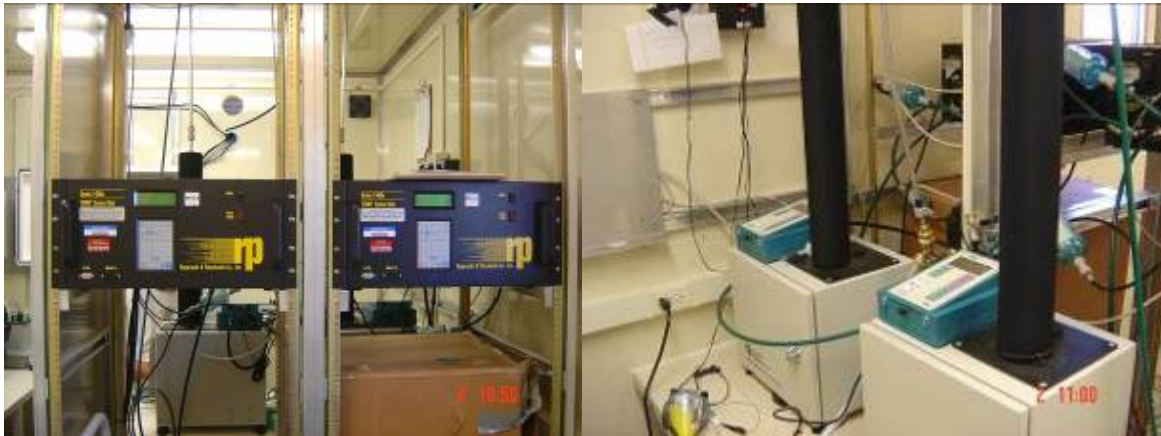
Figure 7.   Left photograph: The front panels of PM$_{10}$ (right on the left photograph) and PM$_{2.5}$ (left on the left photograph) of TEOM. Right photograph: The DUSTTRAK monitors (green) resting on top of the two TEOM measuring units.

       Both PM$_{10}$ and PM$_{2.5}$ DUSTTRAK inlets were attached on a wide "Y" connector, which was connected to one leg of a second "Y" (Figure 8). A funnel with a suction fan was connected to the other leg of the second "Y" to achieve fast exchange of ambient air into the sampling line. Flow calibration and zero-test were performed on the day of installation (May 25, 2007) and subsequent site visits. Deviations in flow were predominantly due to failure of the pump diaphragm. In those cases, the instrument was replaced. Deviations of the zero check were corrected by performing zero calibration according to the manufacturer's operational instruction manual.
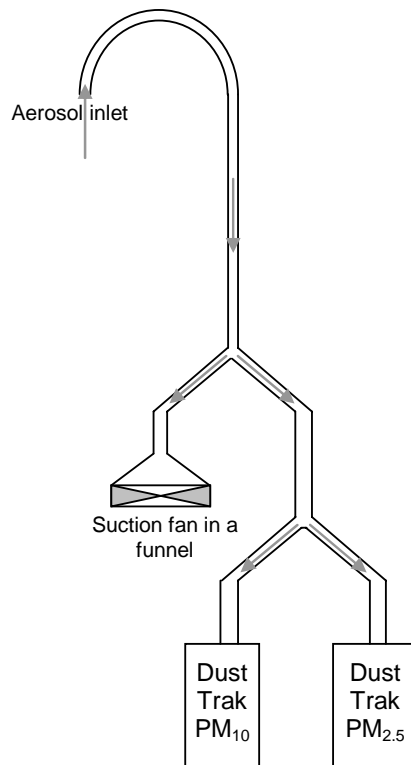
Figure 8.   Schematic drawing of the sampling inlet for the DUSTTRAK (not to scale).

Continuous DUSTTRAK Measurements of PM_{10} and $PM_{2.5}$

Trends and correlations of particle mass are examined using hourly DustTtak data integrated for 24 hours (from 0:00. to 23:59). Statistics of 24-h particle mass are presented in Table 4.

Table 4. Statistics for 24-h PM_{10} and $PM_{2.5}$ mass concentrations.

	Mean	Median	Minimum	Maximum	Std. Deviation
PM_{10}	102.84	70.92	0.30	1,001.00	156.09
$PM_{2.5}$	24.01	10.58	0.05	541.60	32.50

Twenty-four-hour PM_{10} levels ranged from 0.30 to 1,001.0 $\mu g/m^3$, with a mean of 102.84 (s=156.09) $\mu g/m^3$, while $PM_{2.5}$ concentrations varied from 0.05 to 541.60 $\mu g/m^3$, with a mean of 24.1 (s=32.50) $\mu g/m^3$. PM_{10} mass concentrations increased drastically after July 12, 2007. It should be mentioned that the DUSTTRAK (S/N: 85200794) was replaced by another (S/N: 85200795) on July 13, 2007. Given the limitations of DUSTTRAK to measure coarse particles, the intercomparison between filter samples and DUSTTRAK will determine whether variations were caused by atmospheric conditions or not (Figure 9). A consistent relationship between PM fractions was observed before July 12, 2007, with fine particles being accounted for about three quarters of PM_{10} ($PM_{2.5}/PM_{10}$ ratio of 0.75) and about 10 percent for the remaining period (Figure 10). All the operating parameters (flow and zero) were within the acceptable ranges (flow: 1.7 ± 0.1 liters/min and Zero: 0.000 ± 0.001 mg/m^3). While differences in particle mass for weekdays/weekends were not statistically significant, somewhat higher PM_{10} levels were measured on Monday (Day#1) and Tuesday (Day #2) (Figure 11).
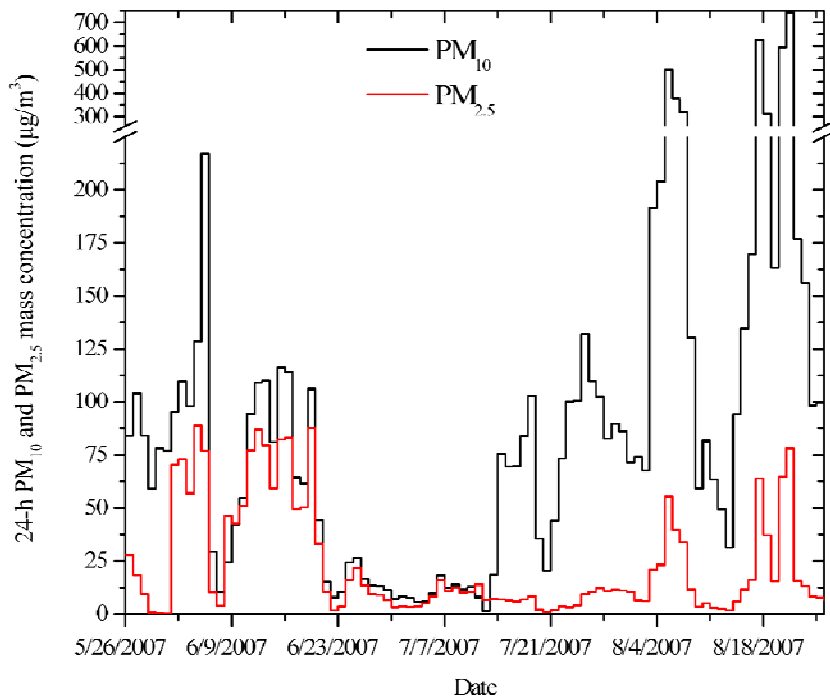
Figure 9.   Mean 24-h PM_{10} and $PM_{2.5}$ mass concentrations measured by DUSTTRAK at Site #7 (Crater Flat).
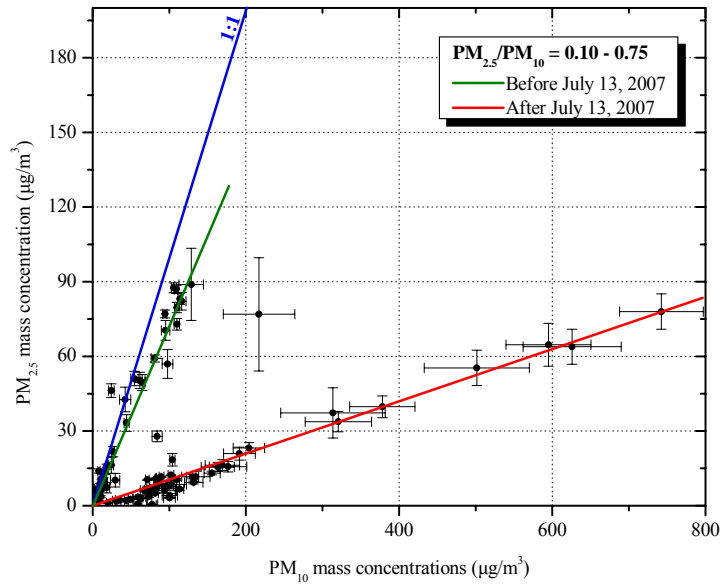

Figure 10. $PM_{2.5}/PM_{10}$ mass ratios at Site #7 (Crater Flat) Error bars represent the standard error of the mean.
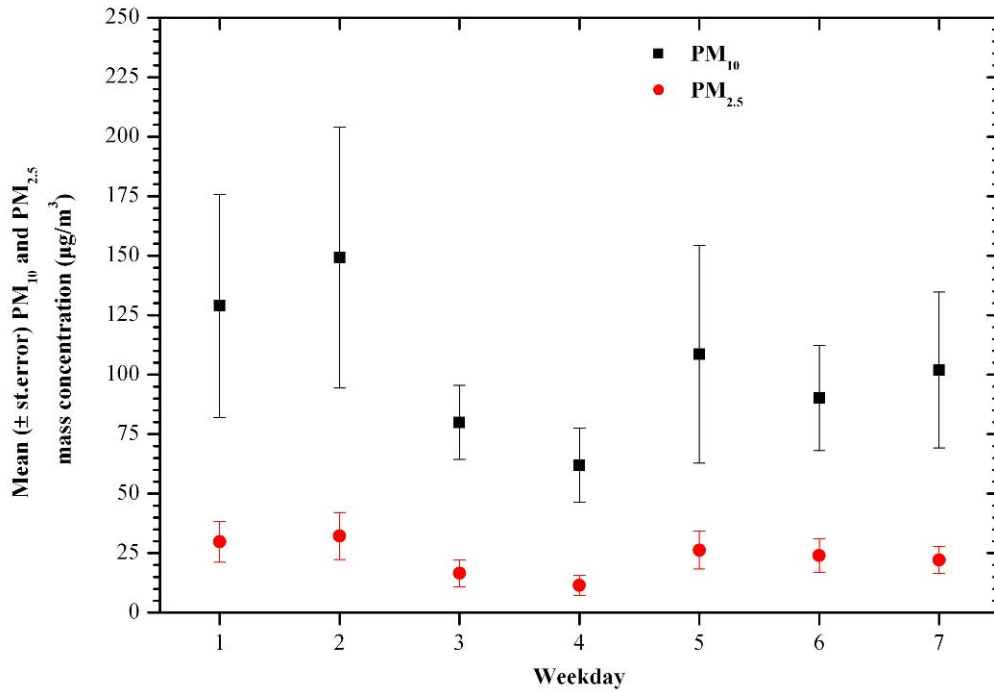

Figure 11. Variation of mean (± st.error) PM_{10} and $PM_{2.5}$ ($\mu g/m^3$) in weekdays and weekends at Site #7 (Crater Flat) (Monday=1, Tuesday=2, Wednesday=3, Thursday=4, Friday=5, Saturday=6, Sunday=7).

<u>Comparison of Filter to Continuous Results</u>

Figure 12 and Figure 13 show the relationships between PM_{10} and $PM_{2.5}$ measured by DUSTTRAK and filter-based methods. The correlations between PM measurements by DUSTTRAK and filter methods were poor, with correlation coefficients of 0.52 for PM_{10} and 0.206 for $PM_{2.5}$. The slopes for PM_{10} and $PM_{2.5}$ measured by DUSTTRAK were 7.46505 and 1.99644, respectively, while high intercepts are computed. The poor correlation for PM_{10} may be attributed to the low range of filter-based values (10 to 20 $\mu g/m^3$).
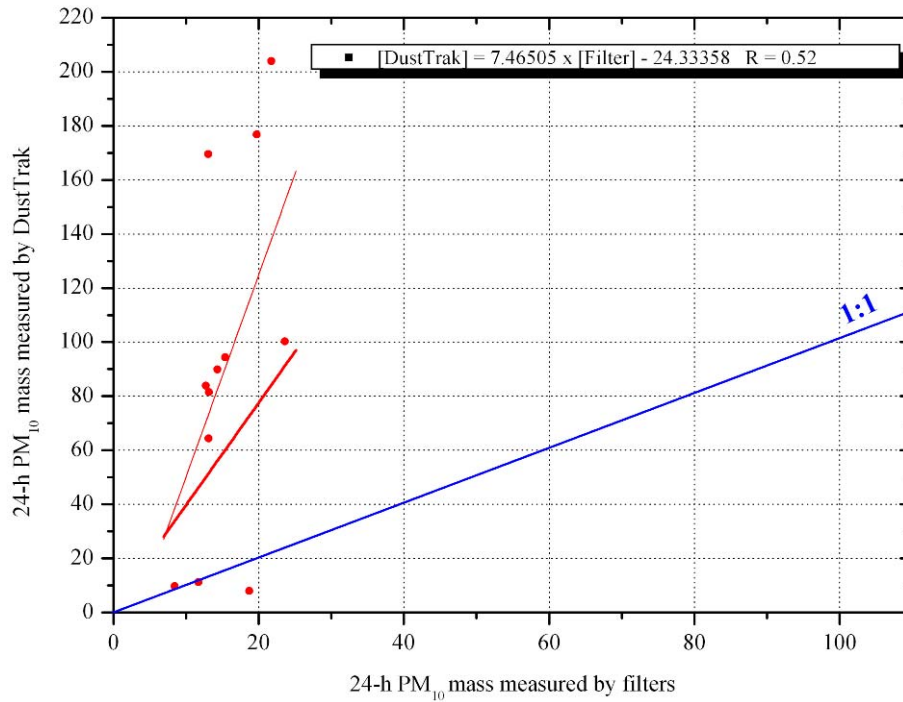

Figure 12. Relationships between PM_{10} concentrations ($\mu g/m^3$) measured by DUSTTRAK, and filter-based methods.
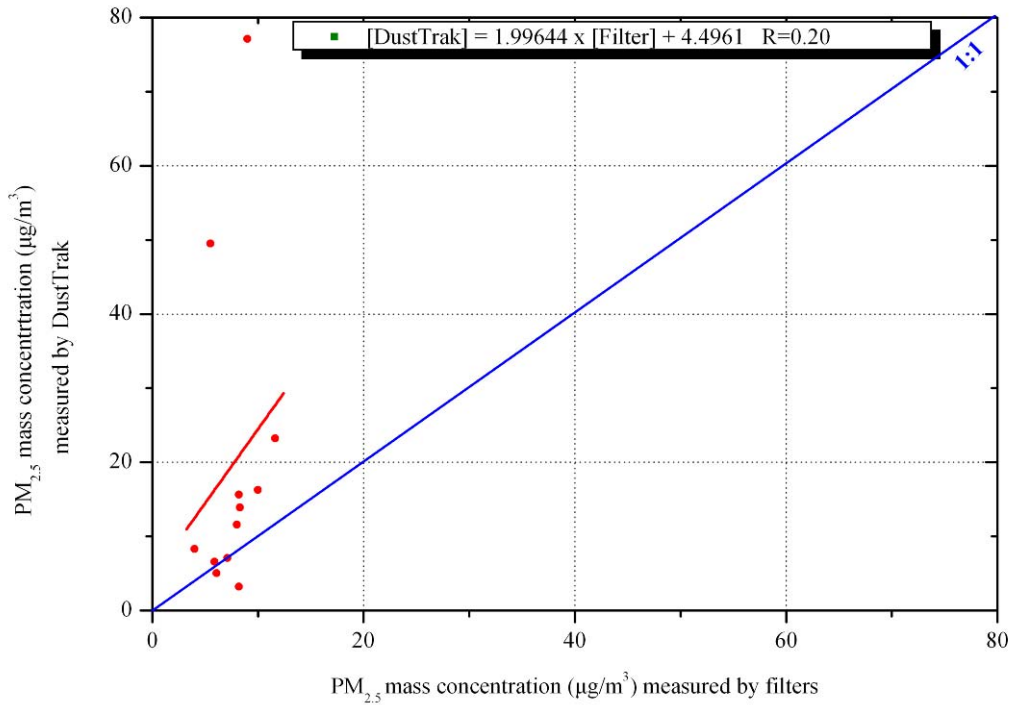
Figure 13. Relationships between PM$_{2.5}$ concentrations (μg/m^3) measured by DUSTTRAK, and filter-based methods.

METEOROLOGY

Variations of hourly data for each meteorological parameter are presented in Figure 14 through 17. Descriptive statistics of hourly data also are presented in Table 5. Solar radiation progressively increased up to 87.4 watts/m^2 (Figure 14). Ambient temperature varied from 50.2 to 109.5ºF with a mean temperature of 86.0ºF for the monitoring period (Table 5; Figure 15). Relative humidity remained lower than 60 percent. No rainfall events were recorded.

Table 5.   Descriptive statistics of 1-hour meteorological data.

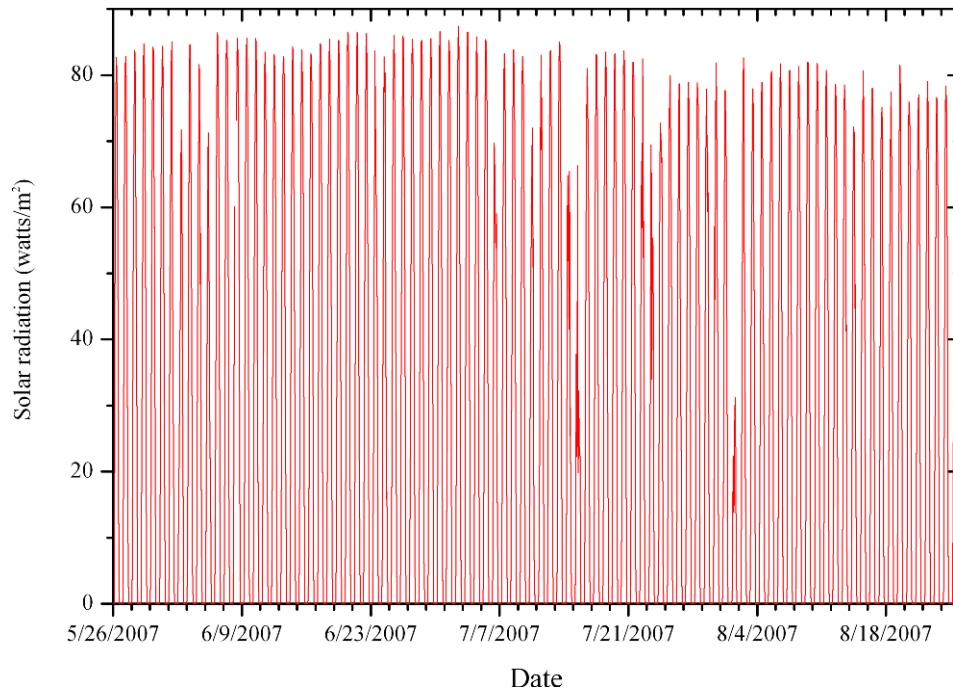|	Mean	Minimum	Maximum
Solar radiation (watts/m^2)	28.0	0.0	87.4
Wind speed (miles/h)	9.4	0.0	33.1
Temperature (ºF)	86.0	50.2	109.5
Relative humidity (%)	14.5	2.9	58.2

Figure 14. Solar radiation (in watts/m^2) at Site #7 (Crater Flat).
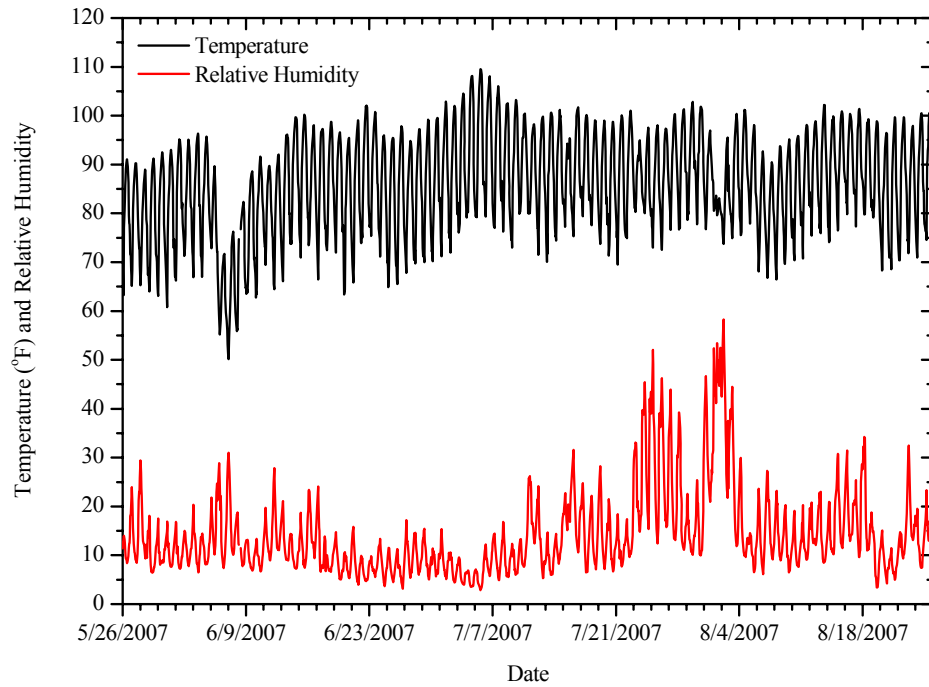

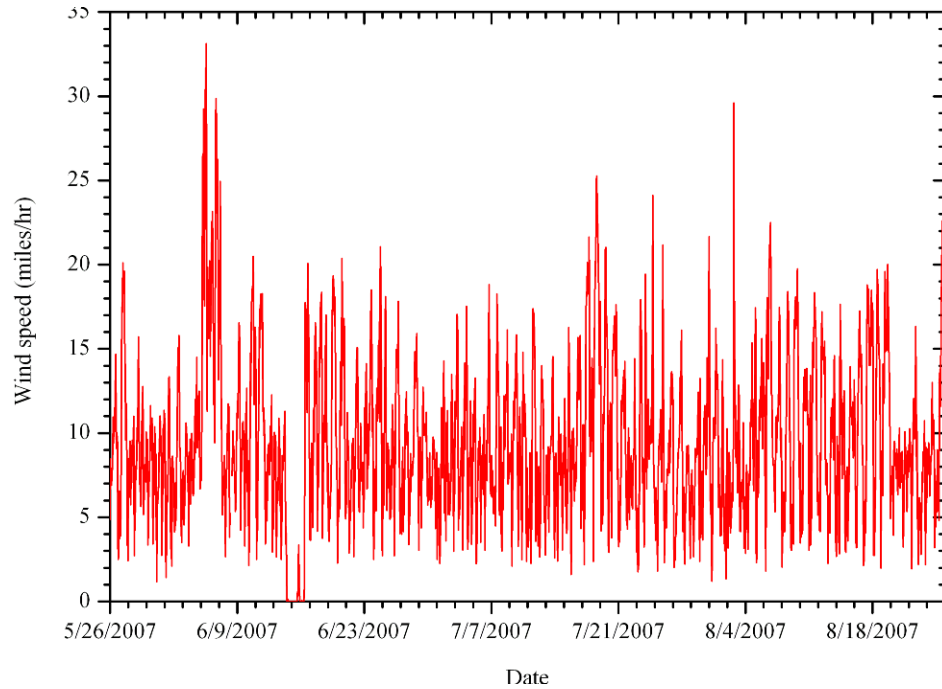Figure 15. Temperature (in ºF) and relative humidity at Site #7 (Crater Flat).

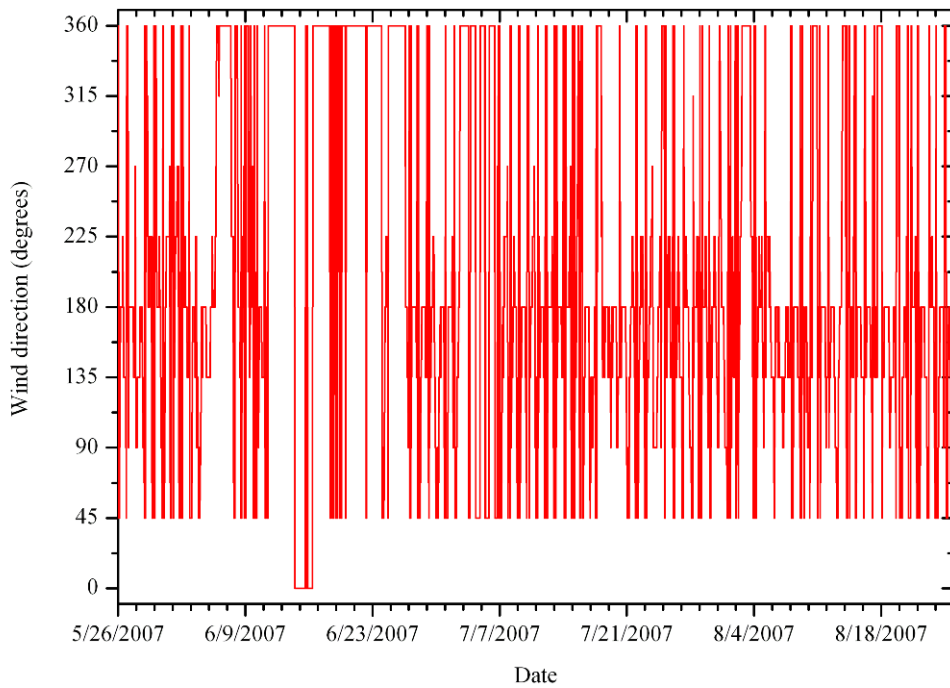Figure 16. Wind speed (in miles/hr) at Site #7 (Crater Flat).

Figure 17. Wind direction at Site #7 (Crater Flat).

Wind conditions for the monitoring period were described by northerly winds during the night and southerly winds during the day, with wind speeds mostly in the range of 5 to 15 miles/hour (Figure 16 and Figure 17). The classification of wind conditions (Table 6) was

retrieved from the Federal Meteorological Handbook. The mean wind speed for each direction bin (8 bins) is presented in Figure 18.

Table 6.   Wind condition classifications.

Miles/hour	Specification
<1	Calm; smoke rises vertically.
1 to 5	Direction of wind shown by smoke drift not by wind vanes. Wind felt on face; leaves rustle; vanes moved by wind.
5 to 9	Leaves and small twigs in constant motion; wind extends light flag.
9 to 14	Raises dust, loose paper; small branches moved.
14 to 23	Small trees in leaf begin to sway; crested wavelets form on inland waters. Large branches in motion; whistling heard in overhead wires; umbrellas used with difficulty.
23 to 35	Whole trees in motion; inconvenience felt walking against wind. Breaks twigs off trees; impedes progress.
35 to 48	Slight structural damage occurs. Trees uprooted; considerable damage occurs.
>48	Widespread damage.

(retrieved from Federal Meteorological Handbook; Chapter 5. Wind;
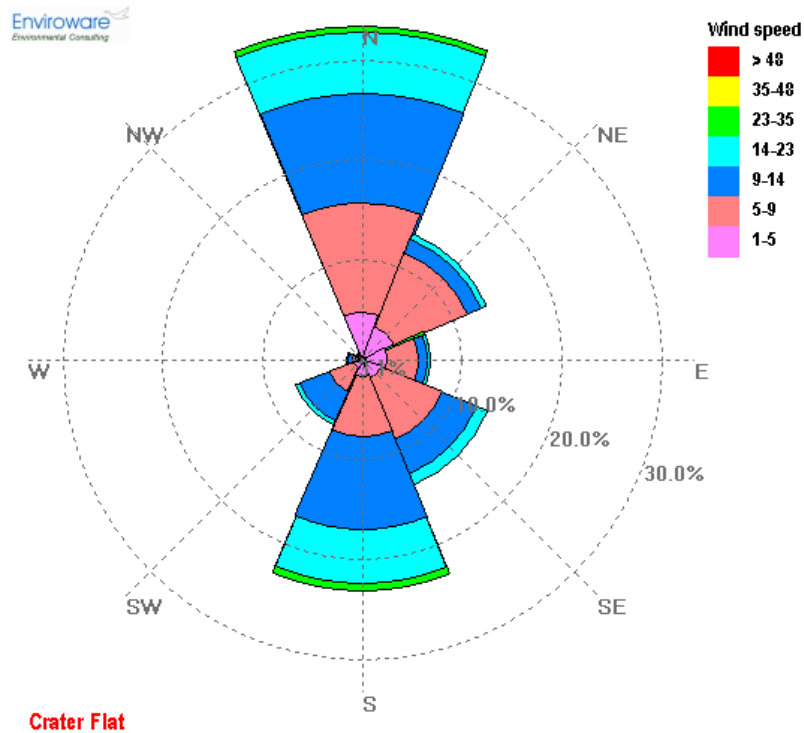*http://www.nws.noaa.gov/oso/oso1/oso12/fmh1/fmh1ch5.htm#chp5link*)

Figure 18. Wind direction and speed at Crater Flat.

On average, winds blowing from south were slightly stronger (11.5 miles/hr) than those from the north (9.6 miles/hr). This is controlled by the north-south-trending topography of the region. Lower wind speeds are recorded for winds blowing from the northwest (Figure 19).
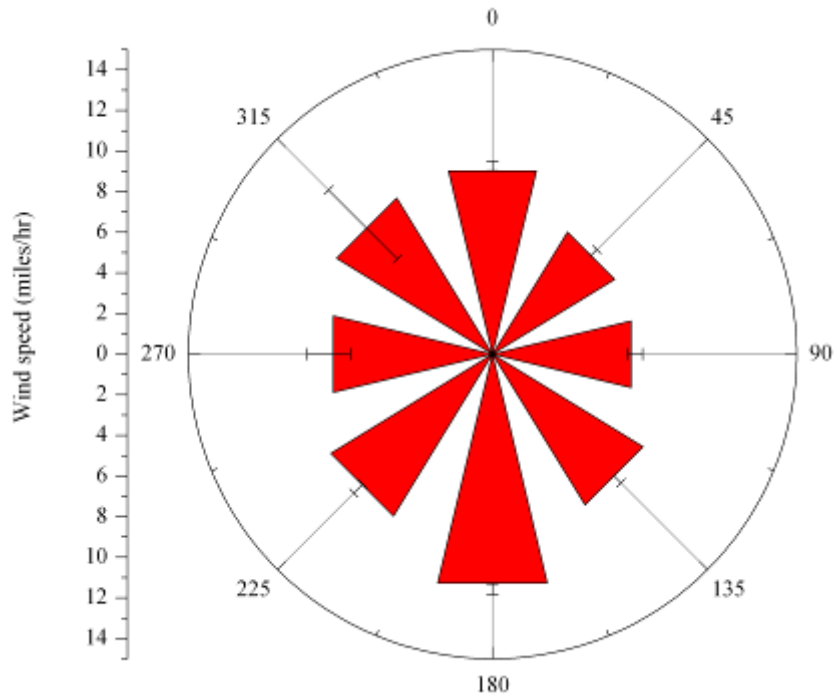

Figure 19. Average wind speed for each wind direction sector. Error bars represent the standard error of the mean.

Relationships of Meteorology with Aerosol Measurements

Trends and correlations of PM mass with meteorological conditions are shown for hourly DUSTTRAK data. A weak bimodal pattern is observed for both fractions of particle mass (Figure 20). The first mode is associated with comparatively higher particle mass concentration in early morning (7:00 to 9:00 for PM_{10} and 10:00 to 11:00 for $PM_{2.5}$) followed by a gradual decrease. The second mode for PM_{10} can be observed in early afternoon (13:00 to 15:00) as winds were increasing, followed by an increase in the evening (19:00 to 22:00). There are significant differences of PM_{10} and $PM_{2.5}$ concentrations for different wind directions, with highest PM_{10} levels for northwest winds, and highest $PM_{2.5}$ levels for northerly winds (Figure 21 and Figure 22).
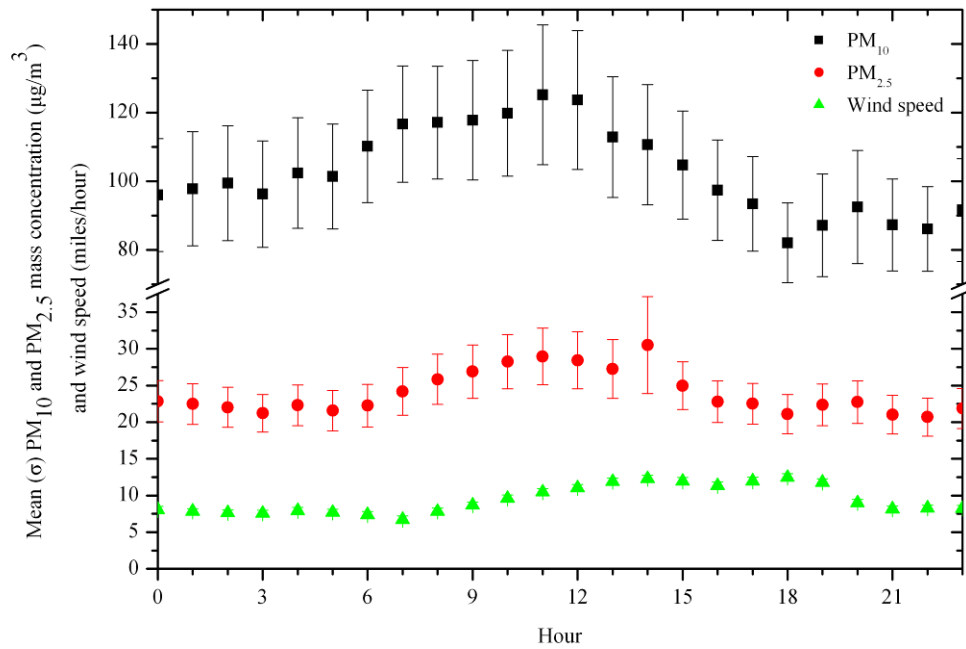
Figure 20. Hourly variation of PM_{10} and $PM_{2.5}$ mass concentrations ($\mu g/m^3$) as well as wind speed (miles/hour) at Site #7 (Crater Flat). Error bars represent the standard error of the mean.

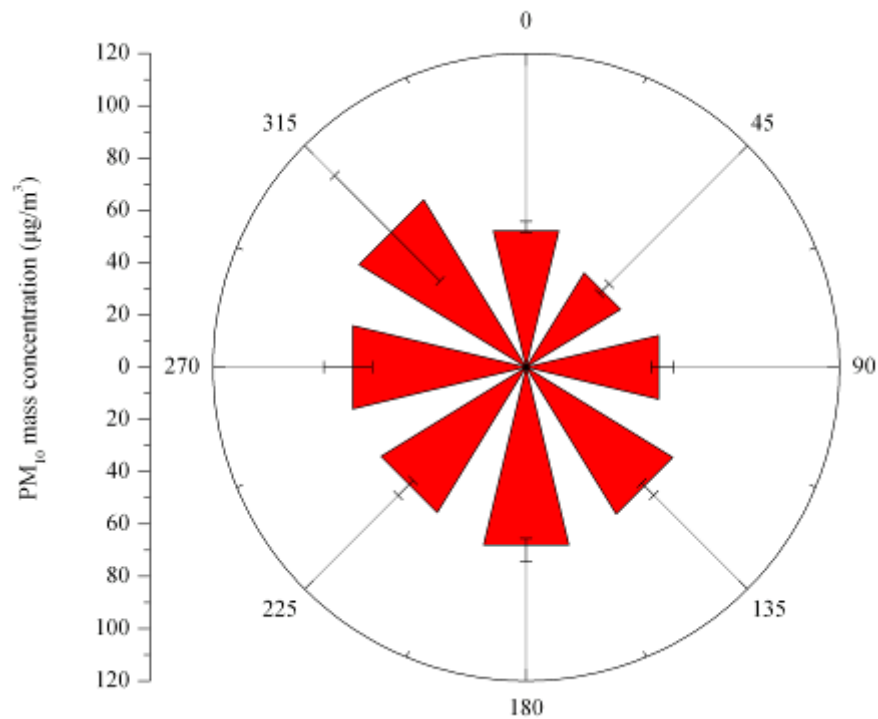Figure 21. Mean ($\pm$ st.error) of PM_{10} mass concentrations ($\mu g/m^3$) for different wind direction sectors at Site #7 (Crater Flat).
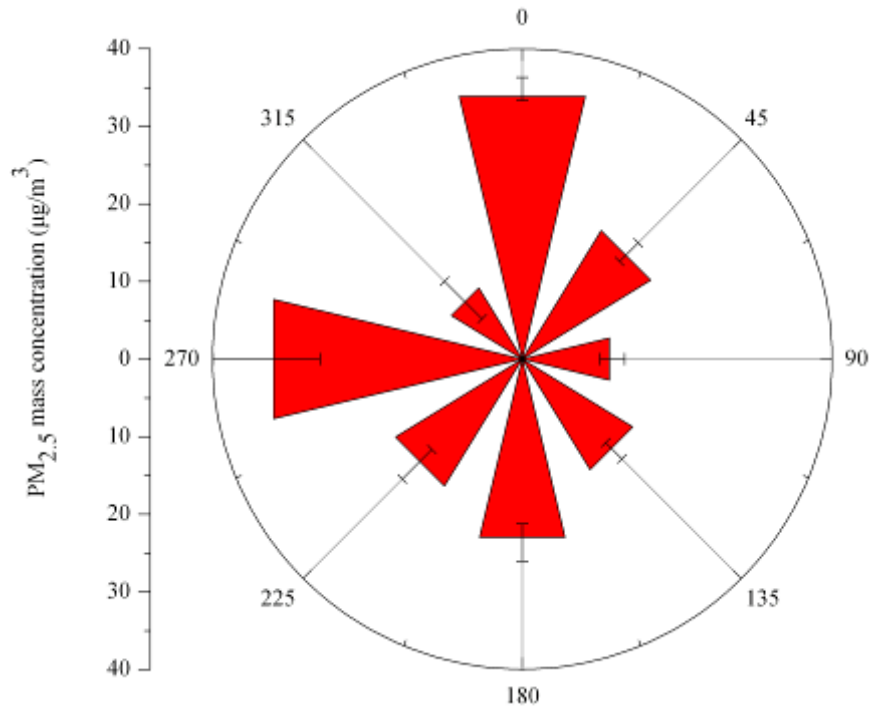
Figure 22. Mean (± st.error) of PM$_{2.5}$ mass concentrations (μg/m^3) for different wind direction sectors at Site #7 (Crater Flat).

CONCLUSIONS

PM$_{10}$ and PM$_{2.5}$ mass concentrations and meteorological conditions were continuously monitored in Crater Flat, from May 25 to August 29, 2007. Because of the remote location of the site, and reliance only on 12-volt batteries and solar power, continuous measurements of PM$_{10}$ and PM$_{2.5}$ were obtained using only DUSTTRAKs, not TEOMs. At the same time, integrated samples of PM$_{10}$ and PM$_{2.5}$ were collected using FRM samplers on a 1-to-6-day schedule. Two sets of filters (June 05 and July 29, 2009) were analyzed for major anions (sulfate, nitrate, chloride) and cations (sodium and potassium), 40 elements (from sodium to uranium), and elemental and organic carbon. The comparison of PM$_{10}$ and PM$_{2.5}$ mass concentrations obtained by continuous monitors and filters showed that differences are associated with the limitations of the operating principle. For example, while light scattering (the measurement technique for DUSTTRAK) is not influenced by volatilization losses and is accurate for fine particles, it performs poorly for coarse particles, resulting in underestimation of PM$_{10}$ mass. PM$_{2.5}$ mass measurements obtained by DUSTTRAK, and filter-based methods were also compared.

Mean 24-h concentrations (measured by DUSTTRAK) of PM$_{10}$ and PM$_{2.5}$ mass were 58.4 and 24.1 μg/m^3, which are lower than the 24-h and annual NAAQS standards (24-h PM$_{10}$: 150 μg/m^3, 24-h PM$_{2.5}$: 35 μg/m^3). Particle mass measured on filters varied from 1.5 to 217.1 μg/m^3 for PM$_{10}$ and from 0.2 to 88.9 μg/m^3 for PM$_{2.5}$. Substantially higher PM$_{10}$ and PM$_{2.5}$ levels were associated with increased wind speeds blowing mostly from the north and south. The chemical composition of both PM$_{10}$ and PM$_{2.5}$ samples indicated that soil is the major component of both fractions, while soil contributes more than 50 percent of PM$_{10}$

21

mass. Sulfate and nitrate account for about 10 percent. Increases in PM$_{10}$ and PM$_{2.5}$ mass concentrations are associated with higher concentrations of soil material.

ACKNOWLEDGEMENTS

REFERENCES

Engelbrecht, J.P., I.G. Kavouras, D. Campbell, S.A. Campbell, S. Kohl, and D. Shafer, 2007a. Yucca Mountain Environmental Monitoring Systems Initiative. Air Quality Scoping Study for Ash Meadows National Wildlife Refuge, Nevada. Letter Report DOE/NV/26383-LTR2007-01

Engelbrecht, J.P., I.G. Kavouras, D. Campbell, S.A. Campbell, S. Kohl, and D. Shafer, 2007b. Yucca Mountain Environmental Monitoring Systems Initiative. Air Quality Scoping Study for Beatty, Nevada. Letter Report DOE/NV/26383-LTR2007-02

Engelbrecht, J.P., I.G. Kavouras, D. Campbell, S.A. Campbell, S. Kohl, and D. Shafer, 2007c. Yucca Mountain Environmental Monitoring Systems Initiative. Air Quality Scoping Study for Rachel, Nevada. Letter Report DOE/NV/26383-LTR2007-03

Engelbrecht, J.P., I.G. Kavouras, D. Campbell, S.A. Campbell, S. Kohl, and D. Shafer, 2007d. Yucca Mountain Environmental Monitoring Systems Initiative. Air Quality Scoping Study for Sarcobatus Flats, Nevada. Letter Report DOE/NV/26383-LTR2007-04

Kavouras, I.G., V. Etyemezian, D. DuBois, J. Xu, M. Pitchford, and M. Green, 2005. Assessment of the Principal Causes of Dust-Resultant Haze at IMPROVE Sites in the Western United States. Final report to Western Regional Air Partnership (www.coha.dri.edu/dust).

Lefer, B.L. and R.W. Talbot, 2001. Summertime measurements of aerosol nitrate and ammonium at a northeastern U.S. site. *Journal of Geophysical Research,* 106, 20,365 – 20,378.

Malm, W.C., B.A. Schichtel, R.B. Ames, and K.A. Gebhart, 2002. A 10-year spatial and temporal trend of sulfate across the United States. *Journal of Geophysical Research,* 107, 4627, doi:10.1029/2002JD002107.

Malm, W.C., B.A. Schichtel, M.L. Pitchford, L.L. Ashbaugh, and R.A. Eldred, 2004. Spatial and monthly trends in speciated fine particle concentration in United States. *Journal of Geophysical Research*, 109, D03306, doi:10.1029/2006JD003739.

White, W.H. and P.T. Roderts, 1977. On the nature and origins of visibility-reducing aerosol in the Los Angeles air basin. *Atmospheric Environment*, 11, 803-812.